



HAL
open science

TALOS: A new humanoid research platform targeted for industrial applications

Olivier Stasse, Thomas Flayols, Rohan Budhiraja, Kevin Giraud-Esclasse, Justin Carpentier, Andrea del Prete, Philippe Souères, Nicolas Mansard, Florent Lamiraux, Jean-Paul Laumond, et al.

► To cite this version:

Olivier Stasse, Thomas Flayols, Rohan Budhiraja, Kevin Giraud-Esclasse, Justin Carpentier, et al.. TALOS: A new humanoid research platform targeted for industrial applications. International Conference on Humanoid Robotics, ICHR, Birmingham 2017, Nov 2017, Birmingham, United Kingdom. hal-01485519v1

HAL Id: hal-01485519

<https://hal.science/hal-01485519v1>

Submitted on 8 Mar 2017 (v1), last revised 9 Feb 2018 (v2)

HAL is a multi-disciplinary open access archive for the deposit and dissemination of scientific research documents, whether they are published or not. The documents may come from teaching and research institutions in France or abroad, or from public or private research centers.

L'archive ouverte pluridisciplinaire **HAL**, est destinée au dépôt et à la diffusion de documents scientifiques de niveau recherche, publiés ou non, émanant des établissements d'enseignement et de recherche français ou étrangers, des laboratoires publics ou privés.

TALOS: A new humanoid research platform targeted for industrial applications

O. Stasse¹ and T. Flayols¹ and R. Budhiraja¹ and K. Giraud-Esclasse¹ and
J. Carpentier¹ and A. Del Prete¹ and P. Souères¹ and N. Mansard¹ and
F. Lamiroux¹ and J.-P. Laumond¹ and L. Marchionni² and H. Tome² and F. Ferro²

Abstract—The upcoming generation of humanoid robots will have to be equipped with state-of-the-art technical features along with high industrial quality, but they should also offer the prospect of effective physical human interaction. In this paper we introduce a new humanoid robot capable of interacting with a human environment and targeting a whole range of industrial applications.

This robot is able to handle weights of 6 Kg with an out-stretched arm, and has powerful motors to carry out movements unavailable in previous generations of humanoid robots. Its kinematics has been specially designed for screwing and drilling motions. In order to make interaction possible with human operators, this robot is equipped with torque sensors to measure joint effort and high resolution encoders to measure both motor and joint positions.

The humanoid robotics field has reached a stage where robustness and repeatability is the next watershed. We believe that, this robot has the potential to become a powerful tool for the research community to successfully navigate this turning point, as the humanoid robot HRP-2 was in its own time.



Fig. 1. Pyrene the first robot of the TALOS serie built by PAL-Robotics.

I. INTRODUCTION

The Darpa Robotics Challenge (DRC) was motivated by the design of several high performance humanoid robots such as ATLAS, or LOLA [1]. It has led to the design of new powerful robots such as Walkman [2], S-One/JAXON [3], PROXI/DURUS [4], [5] and the upgrade of standard platforms such as HRP-2 with HRP-2 Kai [6] or HUBO with DRC-HUBO+ [7]. Following the example of the initial Darpa Challenge on autonomous cars, it is interesting to investigate now the possible industrial outcome of the technologies developed for this competition and to integrate some of the hard lessons learned on this occasion. To realize such investigation, the difficulty is to find an available prototype of humanoid robot that integrates the recent technologies. In this paper, we are presenting such a humanoid robot called Pyrene and depicted in Fig. 1, resulting from the collaboration of a robotics company and a research team. In the rest of the paper, humanoid robots designed before the DRC are considered as belonging to the previous generation, whereas robots build, or used, after or during the DRC are considered as part of the new generation.

A. Availability of recent humanoid robot technologies

A first need is to have actuators providing at the same time high torques and high speed. More specific examples are given in the paper to quantify clearly the needs for possible industrial applications. But in general, if a humanoid robot has to perform a reactive motion to keep balance, it needs to perform fast motions with high torques. Following the arguments of Engelsberger and al. [8] the Atlas robot is providing high torque with high bandwidth but it is extremely noisy, needs high power and has unmodeled friction/stiction making the control not so easy. In addition it is potentially risky when evolving in environment with humans. For this reason it is very unlikely that this robot will be certified as a collaborative robot.

On the other hand the seminal work of Urata [9], leading to the design of the S-one robot from Schaft, shows that it is possible to realize powerful motions with electric motors. WALK-MAN [2] and DRC-HUBO+ [7] are robots using this kind of technology. WALK-MAN has new high performance actuators with impressive capabilities, but it is a laboratory prototype and the maintenance and support are difficult to perform outside IIT. The DRC-HUBO+ as well as the HRP-2 Kai have two motors in parallel, which are increasing the torque capabilities but not the speed. In addition the DRC-

*This work was supported by the ERC Grant ACTANTHROPE

¹ CNRS - LAAS, Toulouse, France, ostasse@laas.fr

² PAL - Robotics, Barcelona, Spain
francesco.ferro@pal-robotics.com

HUBO+ is using CAN bus, which is a bottleneck if one wants to have a 1 KHz access to the low level controllers. To mitigate this problem, recent robots are using EtherCAT (HRP-2 Kai and WALK-MAN) for their communication bus.

Humanoid robots such as Valkyrie [10] or WALK-MAN [2] are using Serial Elastic Actuators (SEA). The interest of such devices are their capabilities to absorb impact, store the related energy and release it later on. In addition the spring can be used as a measurement device of the torque. However it complexifies the robot control as the actuator dynamics needs to be taken into account [11].

Torque controlled robots such as TORO [8] or DURUS [5] are very promising to deal with unplanned contact with the environment and humans. Unfortunately TORO is unlikely to be available outside DLR. Recent robots such as REEM-C have encoders at the motor side as well as at the joint side. Provided that the encoder resolution at the joint side is sufficient, it is possible to use them to model the deflection induced by the harmonic drive. This deflection is then an image of the torque.

DURUS is another new humanoid robot sold by SRI with impressive efficiency capacities with springs at the ankles and torque control. The transmission has been designed to have low friction, and the robot has torque sensing in all the joints. However, if the spring constrained along the vertical axis at the ankles is efficient to store energy and absorb impacts, its implication during manipulation is less clear. Our experience on several applications is that humanoid robots are usually used in acyclic behaviors, and mix high-stiffness control (for manipulation and support legs) with low-stiffness control (for landing and human-robot interaction). A mechanical compliance useful during low-stiffness control then needs to be dealt with during high-stiffness behavior by the control architecture, and usually imposes a compliance higher than using a pure rigid system. Therefore the approach for Pyrène was to have a controlled compliance, and not a mechanical one.

As torque control is still a research topic, Pyrène allows for both position and torque control.

Finally the recent advances on wholebody control rely mostly on complex optimization problems solved in an efficient manner [12], [13], [14], [15]. This involves a significant computational power available on the robot.

B. Applications

In this paper, we are focusing mostly on scenarios coming from Aircraft manufacturing. The most common behaviors that have to be implemented in this context are drilling and screwing. This imposes to have a robot able to handle tools weighting up to 6 Kg with stretched arms. The environments in which the robot has to evolve include narrow spaces and stairs, similar to the ones found in the DRC. Although robots with wheels have already been investigated in Aircraft Industry, they involve the need of elevators and thus increase the cost of their deployment.

As well as in the context of research, an important factor for the deployment of humanoid robots in real scenario is the



Fig. 2. (left) HRP-2 climbing dynamically stairs up to 15cm (right) HRP-2 walking on a beam.

repeatability. This goal can be reached when the design of the robot is done in collaboration with an industrial partner mastering the integration know-how, or with institutes having strong technological centers such as DLR [8] and IIT[2]. The successful production of the HRP series [16], [17], and the robots from Boston Dynamics are good examples of robots with industrial quality. For this reason Pyrène, the robot presented in this paper, was built by the company PAL-Robotics. PAL-Robotics has also successfully realized the REEM-B [18], REEM-C humanoid robots. Pyrène is the first prototype of the TALOS serie. The robot was specified by the Gepetto team of the LAAS-CNRS laboratory based upon its expertise in humanoid robots.

II. FEEDBACK FROM THE KOROIBOT CHALLENGES AND PREVIOUS WORK

In this section we describe the problems and challenges encountered by the Gepetto team in the Koroibot challenge [19], with the humanoid robot HRP-2. In addition we report on problems encountered during a proof-of-concept for an Aircraft manufacturer.

The motions described in this section were realized and evaluated assuming that the geometry of the environment is known a priori and that a real-time planner could provide a plan [20].

We used our implementation of the real-time pattern generator proposed in [21] to compute the Center-of-Mass (CoM) and Center-of-Pressure (CoP) trajectories given the foot-steps plan.

A. Climbing stairs

The stairs considered in this challenge were of two heights: 10 cm and 15 cm , see Fig. 2-(left), with a width of 20 cm . Both the 10 cm and the 15 cm heights need a different timing for the double support and the single support phase with respect to the timing used in flat floor. Indeed, as the trajectory is longer due to the avoidance of the stairs, the velocity limits of the HRP-2 actuators are reached when keeping the same timing as for the flat floor. However, lowering the velocity limits tends to increase the swinging motion

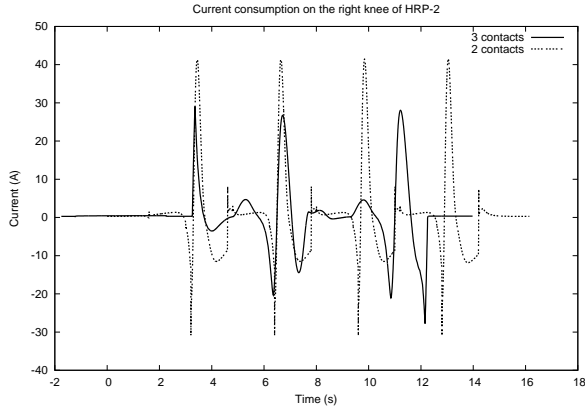


Fig. 3. Current of HRP-2 Knee when climbing stairs with only the feet (2 contacts) or with the feet and the right hand on the handrail (3 contacts)

from one foot to the other, which increases the likelihood of hitting a kinematic limit. The free parameters which can be modified are the feet and CoM height trajectories. The feet and CoM trajectories are however subject to constraints: the take-off and landing phases need to have zero speed, zero acceleration at the beginning and at the end and go through an intermediate point to avoid collision. The CoM height trajectories have less constraints apart the fact that, as [21] assumes a cart-table model, the acceleration has to be very small compared to gravity.

The 15 cm height stairs however made the robot reach another limit related to the batteries. Using the Recursive Newton-Euler Algorithm (RNEA) the joint torques needed to realize the articular trajectories provided by the walking pattern generator were computed. Finally a model of the actuator was used to compute the current needed to generate the motions. The result, shown in Fig. 3, is a peak demand of 40 A, even though the peak current of the batteries is 32 A. In this case, the batteries are playing the role of capacitors by delivering 14 times their nominal current (2.8 A). This problem was solved by using a gait with 3 contacts, including one hand on the handrail, which is more stable and allows to have less consuming feet trajectories [15].

B. Stepping stones

The stepping stones behavior depicted in Fig. 4 bears some similarities with the terrain task of the DRC. As specified in [6], the kinematic limits of HRP-2 are constraining the range of motion, to a weak version of the terrain task. A slight difference between the stepping stones and the terrain task lies in the fact that the stones are supposed to be apart from each other. This imposes large foot-steps. If this is combined with a height difference, the problem of stepping stones can be more difficult than the climbing stairs as the distance between two contacts is larger. The same relationship between the velocity limits, the kinematics



Fig. 4. HRP-2 performs stepping-stones behavior

constraints and the timings found for the climbing stairs behavior appeared in this situation. This limited the height difference between two stepping stones to 5 cm.

C. Walking on a beam

Thanks to its canter-lever structure at the level of the hip, the humanoid robot HRP-2 can easily cross its feet in front of each other, as demonstrated by Kaneko in [22]. We carried out the same experiments as shown in Fig. 2-(right). In a similar manner the timing of the feet had to be slowed down, compared to the initial timing on flat floor. This is again mostly due to the velocity associated to the large steps. This capability is interesting for passing through narrow passage.

D. Reactive walking

Reactive walking is crucial for robots in order to be able to evolve in dynamic environments, for interacting with humans and to recover balance. It is however important, in this case, to be able to generate high accelerations and high speeds. This dual requirement is due to the fact that an abrupt change of the future is generally triggering a high acceleration of the CoM. For a flying foot this involves a high speed, and for the hip motors high torques to handle the change of direction.

E. Screwing

In our screwing behavior the humanoid robot HRP-2 had to use its two grippers to handle the screwdriver provided by our industrial partner. A limitation of the initial HRP-2 comes from its 6 DOFs arm, which are very easy to bring into singularities, or in self-collision. A common solution is to modify the robot arms to add one additional DOF. Another problem is the width of the HRP-2 robot, which is quite large (621 mm) and forbids it to pass through narrow spaces. This is mostly due to its large shoulders, fixed on each side of the robot.



Fig. 5. Pyrene folding its arms in front

	HRP-2 Kai	WALK-MAN	Pyrene	DRC-HUBO+
Height	1.710 [mm]	1915 [mm]	1750 [mm]	1750 [mm]
Width	629 [mm]	815 [mm]	775 mm - 550 [mm]	540 [mm]
Depth	355 [mm]	600 [mm]	330 [mm]	[mm]
Weight	65 Kg	132 Kg	95 Kg	80 kg
DoFs	32	32	32	32
Head	2 D.O.F.	2 D.O.F.	2 D.O.F.	1 D.O.F.
Arm	2 Arms × 7 D.O.F.			
Hand	2 Hands × 1 D.O.F.			
Waist	2 D.O.F.	2 D.O.F.	2 D.O.F.	1 D.O.F.
Legs	2 Legs × 6 D.O.F.			

TABLE I

OVERALL DESCRIPTION OF ROBOTS USED IN THE DRC

III. SPECIFICATIONS OF PYRÈNE

A. Kinematics constraints

1) *Range and overall structure*: Pyrene has almost the same joint range than the classical model of the human structure (see Table. II). Compared to robots of the new generation, Pyrene has a wider range of motions than ATLAS, with the exception of the ankle inversion. Conversely it has a slightly less wide range than WALKMAN for almost all the joints. It has 32 DoFs as most of the recent humanoid robots (see Table. I), such as HRP-2 Kai, WALK-MAN, and DRC-HUBO+. In terms of weight, with 95 Kg Pyrene is heavier than DRC-HUBO+ and HRP-2 Kai, but lighter than WALK-MAN and ATLAS.

2) *Shoulders*: In contrast to HRP-2 and HRP-2 Kai, Pyrene has been designed to have a maximum manipulability in its front in order to perform drilling and screwing motions. For this reason, the first axis of the shoulder, instead of being along the pitch axis, is along the yaw axis. In this way, when both shoulders are folded in the front (see Fig.5) the robot has a width of 550 mm instead of 775 mm. It becomes

Joint	Human body	WALK-MAN	TALOS	ATLAS
Hip pitch	-120.0,+ 10.0	-120.0,+ 60.0	-120.0,+ 45.0	-92.38,+37.68
Hip roll	-40.0,+ 30.0	- 50.0,+ 40.0	-30.0,+ 30.0	-30.0,+30.0
Hip yaw	-35.0,+ 35.0	- 90.0,+ 50.0	-20.0,+ 90.0	-10.0,+45.0
Knee	0.0,+145.0	0.0,+140.0	0.0,+150.0	0.0,+135.0
Ankle pitch	-40.0,+ 15.0	- 80.0,+ 60.0	-75.0,+ 45.0	-57.0,+40.0
Ankle roll	-30.0,+ 30.0	- 45.0,+ 45.0	-30.0,+ 30.0	-45.0,+45.0

TABLE II

JOINT RANGES

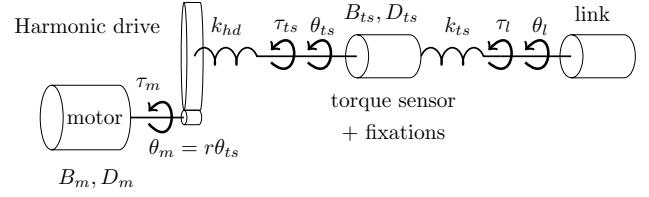


Fig. 6. Structure of Pyrene actuator

then less large than HRP-2 Kai, which has its shoulders along the pitch axis. In addition, the initial HRP-2 had only 6 DoFs in its arms. Thus to control the end-effector in position and orientation only one solution is possible. While this simplifies the computation of the inverse kinematics, it severely limits the manipulability if additional constraints need to be handled. The generalization of numerical methods to deal with the problem of redundancy makes now the interest of analytical solution weaker.

3) *Hip and knee*: From the kinematic viewpoint the cantilever structure of HRP-2 is interesting to alternatively put one foot in front of the other when going through narrow spaces. However, this structure is not ideal for legs with higher-powered motors because it puts more stress on the mechanical structure and increases the width of the robot. For these reasons, the two legs, although close to each other, are designed not to collide while spanning a wide range of motion¹.

B. Batteries

Pyrene is equipped with Li-CNM (Cobalt-Nickel-Manganese) batteries, which are able to deliver 74V DC with a capacity of 15 Ah. Compared to HRP-2 Kai the capabilities of the batteries are 50 % higher. Finally, if powerful motions are needed, the batteries are also able to deliver peaks of 150 A. These capabilities are driven by the work of Urata, which led to the S-One robot [9].

C. Actuators

The structure of Pyrene actuators is depicted in Fig. 6. A brushless motor is connected to a Harmonic Drive (HD), which is itself connected to a torque sensor. Finally the torque sensor is connected to a link. Two high-precision encoders (19 bits) give the motor position, θ_m , and the joint position, θ_l . This relationship gives rise to the following set of equations linking the motion and the motor parameters:

$$\begin{aligned}
 k_{ts}(\theta_{ts} - \theta_l) &= \tau_l \\
 B_{ts}\dot{\theta}_{ts} + D_{ts}\dot{\theta}_{ts} + k_{hd}(\theta_l - \frac{\theta_m}{r}) &= \tau_{ts} \\
 T_{fr}(\tau_m, \tau_l, \theta_m) + B_m\dot{\theta}_m + D_m\dot{\theta}_m - k_{hd}(\frac{\theta_m}{r} - \theta_{ts}) &= K_m i_a \\
 \frac{V}{R} - \frac{K_b}{R}\dot{\theta}_m &= i_a \\
 K_m i_a &= \tau_m
 \end{aligned} \tag{1}$$

where the parameter definitions are given in Table.III.

¹The reader is kindly invited to watch the accompanying video

$k_{ts} \approx 270 \text{ KNm/rad}$	Torque sensor stiffness
$k_{hd} \approx 540 \text{ KNm/rad}$	HD stiffness
$B_{ts} = 0.033 \text{ kgm}^2$	Inertia of the torque sensor
B_m	Motor inertia
$D_{ts} = 0$	Damping of the torque sensor
$D_m = 0$	Motor Damping
T_{fr}	Friction of the HD
$K_m = 0.1$	Motor torque constant
$r = 100$	HD reduction ratio
θ_{ts}	Position of the torque sensor
θ_m	Position of the motor
τ_l	Load torque
$R = 200 \text{ m}\Omega$	Armature resistance
V	Armature Voltage
$K_b = 80 \text{ rpm/V}$	Back-EMF constant
i_a	motor current

TABLE III
ACTUATOR PARAMETERS LIST

This model is very similar to the one found in [23]. In practice we found out on HRP-2 that most of the problems arised from: power limitation ($P = Vi_a$), temperature overheating, limitation in torques from the motor (τ_m) or the HD (τ_{ts}). The maximum peak motor torque given by the data sheet is usually higher than the maximum peak torque for the HD. In addition the peak motor and HD torques can be exceeded during a short time interval. For instance, let us take the biggest HD available in WALKMAN (CPL serie size 25, ratio= 80 according to [24]). According to the datasheet, the momentary peak torque is $255Nm$. This corresponds to the kind of peak torque we have experimented on HRP-2 for high-demanding motions during 10 ms , despite the lower limits of this robot ².

It is more difficult to take into account the torque limits induced by a large torque applied over a longer period of time, or repeatedly. This creates internal temperature built-up. Therefore the torque and the time during which one can apply it depend upon the environment temperature and the past usage of the motor. It is possible to create a model of the motor temperature behavior [25]. The HDs are also subject to time issues as a repeatable peak torque is lower than momentary peak torque. For instance, in the case of the HD example used previously, the repeatable peak torque is 137 NM .

As depicted in Table.IV, Pyrène seems to have lower power and speed than WALKMAN according to [2]. However, looking at [24], which gives a more thorough description of the actuator, one can remark that the numbers given in [2] are computed from the HD reduction ratio, but they do not consider the torque limits of the HD. For this reason three columns are given for Pyrène in Table IV. The first one gives the actuator limit including the HD. The second is obtained considering the max torque that the motors can deliver, the limitations of the maximum current of the motor drives and the maximum momentary peak torques of the HD. The third column considers only the motor limits. The third

column gives numbers higher than WALK-MAN [2], but the first column is similar to the numbers given in [24] where the HD limitations are considered.

Finally ,this actuator allows for both position and torque control.

D. Sensors

1) *IMU and force sensors*: Quite classically Pyrène is equipped with an IMU at the level of its waist. This allows measuring the trunk orientation and the robot global acceleration with respect to the gravity field. In addition Pyrène is also equipped with force sensors at the level of the hands and the feet. The main difference with respect to HRP-2 is the capacity of these force sensors to sustain up to 6 times the weight of the robot, whereas it is 2 times on HRP-2.

2) *Torque sensors*: As mentioned in the paragraph describing the actuators, Pyrène is equipped with torque sensors in almost all the joints, except the two wrist DOFs and the two head DOFs. They are allowing a direct measurement of the torque applied on the load side. We believe that the redundancy of the sensors, as well as their fast update due to the EtherCAT bus, are a key ingredient to achieve torque control on real humanoid robots.

3) *Vision*: Pyrène is equipped with an ORBBEC Astra Pro RGB-D camera. The stairs used as a testbed for developing our algorithms are depicted in Fig. 8. The camera providing the RGB part is a CMOS camera using a rolling shutter system, which can be problematic with dynamic scenes. The head has been designed to be modified, and we plan to add a stereoscopic system, or at least a CCD camera, together with an IMU for latter investigation. Fallon has shown in [26] that an advanced stereoscopic system can be highly reliable.

E. Computational power

The robot is supplied with two computers, each equipped with dual i7 CPU at 2.8 GHz. Each CPU has two cores and is hyper-threaded. However, since the real-operating system used is RT-PREEMPT, only 4 CPUs are available on the control computer. They are anyway available on the computer for vision and high-level computation. The motherboards are in a specific box called the logic box, which can be easily removed. This ensures proper cooling of the CPUs and facilitates their upgrade, a key factor for HRP-2 extended lifespan.

F. Software environment

PAL-Robotics has a history of providing its robots (REEM-C and TIAGO) with ROS deeply integrated. The operating system used in Pyrène is an Ubuntu 14.04 LTS. The robot low-level system is developed with *ros_control*. The robot can be simulated with Gazebo, and the multimedia system is using the stacks providing navigation and map-building.

²We are unfortunately not able to provide the exact limits of the HRP-2 robot due to a Non-Disclosure Agreement.

Joint	WALK-MAN		TALOS		Atlas	
	Torque Max	Speed	Torque Max	Speed	Torque Max	Speed
Hip flex./extension/pitch	400 Nm	9 rad/s	157 Nm / 284 Nm / 400 Nm	8.58 rad/s	260 Nm	12 rad/s
Hip abduction/adduction/roll	400 Nm	8.2 rad/s	157 Nm / 284 Nm / 404 Nm	8.58 rad/s	90 Nm	12 rad/s
Hip rotation/yaw	140 Nm	19.5 rad/s	82 Nm / 147 Nm / 210 Nm	5.86 rad/s	110 Nm	12 rad/s
Knee	400 Nm	16.2 rad/s	308 Nm / 465 Nm / 648 Nm	8.58 rad/s	890 Nm	12 rad/s
Ankle plantar/dorsi flexion/pitch	330 Nm	18.6 rad/s	157 Nm / 284 Nm / 400 Nm	8.58 rad/s	220 Nm	12 rad/s
Ankle inversion/eversion/roll	210 Nm	16.7 rad/s	82 Nm / 147 Nm / 232 Nm	8.58 rad/s	90 Nm	12 rad/s

TABLE IV
TORQUE AND SPEED RANGES FROM [2].

1) *roscontrol*: *roscontrol* is an abstract interface that allows to switch easily from simulation to real tests on the robot. The same is true for Pyrène, but the robot has additional joint state information that needs an extension of the interface. Therefore the robot is now working on a modified version of the main stream *roscontrol* and we hope to submit this modification in order to keep the compatibility with the system. More precisely, according to the model presented in Eq. 1, we need an interface to measure the joint position at the load side θ_l (not provided by *roscontrol*) and the motor side θ_m (provided by *roscontrol*). We also need the motor current i_a (provided by *roscontrol*) and the torque sensor τ_{ts} (not provided by *roscontrol*). Thanks to *roscontrol* we were able to port the Stack Of Tasks [27], our software control architecture in less than a month.

roscontrol is easier to use than the OpenRTM architecture, however it currently lacks the composability offered by OpenRTM [28]. For instance, the stabilizer, the walking pattern generator and a dynamical library are provided as basic software bricks through OpenRTC components.

2) *Simulation*: Several simulators are available under ROS, but not all of them are compatible with *roscontrol*. Gazebo is the simulator widely used in the robotics community as it is a *system simulator* which makes it possible to test a large software framework. However, Gazebo is mostly relying on the ODE dynamic engine. Even if recent developments considerably improved the reliability of this engine for simulating dynamics quantities, it still suffers from problems to simulate biped robot walking. Indeed spurious forces introduced by a lack of priority between the constraints related to the robot mechanical structure and the contacts with the environment are leading to unstable or unrealistic simulations. In our experience, OpenHRP/AIST dynamical engine provides a better result because the rigidity of the mechanical structure is guaranteed by use of Spatial Algebra computation for the kinematic tree of the robot. When the dynamics of the robot is computed, it is then included in a global dynamical system with general coordinates and contact-force detection. Regularization is achieved indirectly by introducing spring joints only in the parts of the system that are flexible. For instance, in HRP-2, there is a bush-rubber between the robot ankles and soils. Using this approach, the OpenHRP simulator together with HRP-2 has constantly provided us with meaningful simulations. We are currently working on a version tailored to the Pyrène robot. In the meantime, for motions that are not highly dynamics

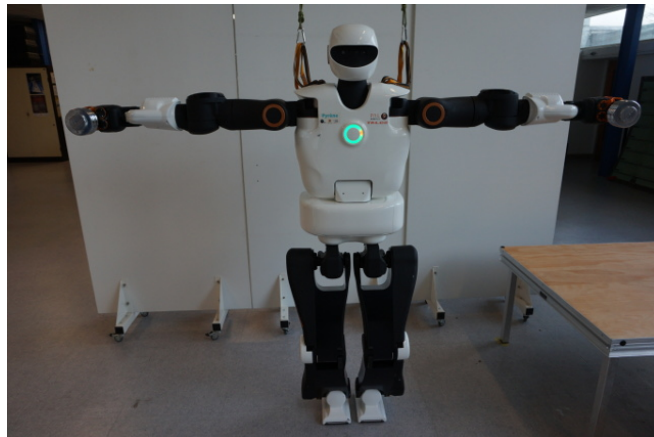


Fig. 7. Pyrène is holding two weights of 6 Kgs in each gripper with stretched arms.

(e.g. moving slowly while standing), the dynamic simulation provided by Gazebo/ODE is sufficient.

IV. SIMULATIONS AND EXPERIMENTS

In this section, the robot has been controlled using position control. The implementation of torque control is left for future work.

A. Experiments

1) *Stretched arms*: We have performed tests where the robot is holding a weight of 6 kg with each gripper with stretched arms, as depicted in Fig. 7. The actuator along the shoulder roll axis reached 75% of its maximum torque, with a slight bending at the shoulder and at the wrist.

2) *Walking*: Pyrène is supplied with the same walking pattern generator used for REEM-C. Fig. 9 depicts the robot walking with bricks in its hand. We kindly invite the interested reader to go at the following url to have a demonstration of the robot capabilities: <https://youtu.be/SxdNvP2jKcc>. The concept of this walking pattern generator is very similar to the one proposed in [21]. It does not use a dynamical model to filter the discrepancy between the inverted pendulum model and the momenta generated by the limbs during the motion. However, because it provides a fast analytical solution, the system is able to modify online its foot-steps according to the feedback of the CoP computed from the force-torque sensors available on both feet³. The

³Several other methods using analytical solutions have been proposed in the past decade, due to space constraints we cannot list them all here

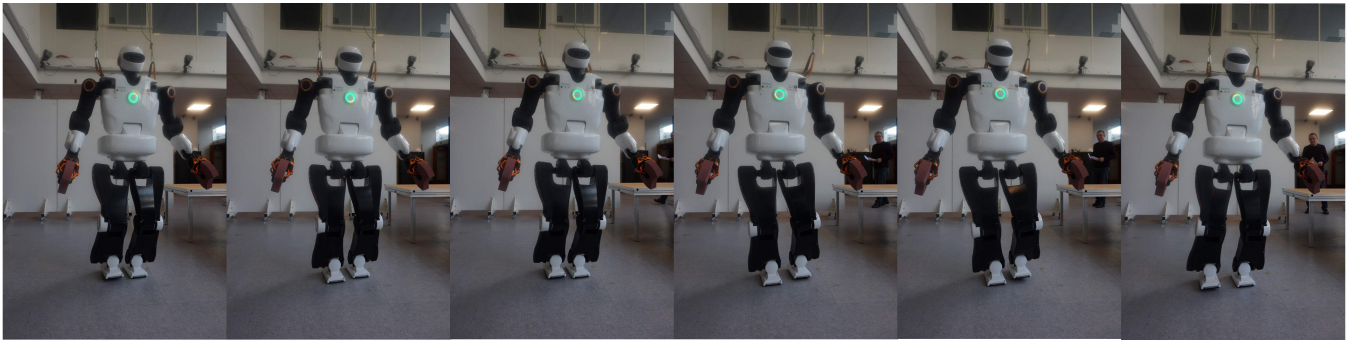


Fig. 9. Pyrene walking with bricks in both grippers. Each brick weight 1.5 Kg

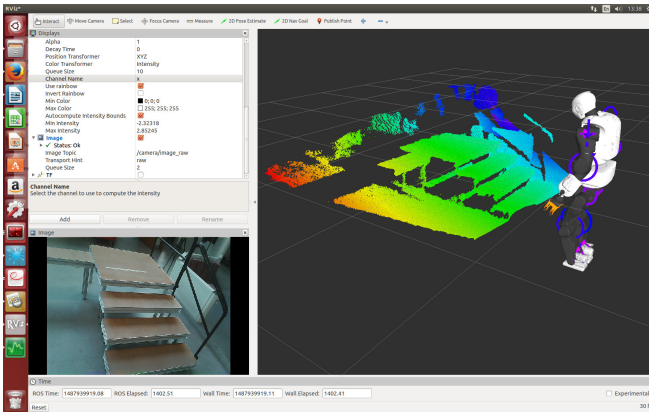


Fig. 8. View of the robot image and its RGB-D camera. The values of its torque sensors are also displayed

walking is therefore very reactive and can be used with a joystick. We plan to improve this algorithm by using a method coupling dynamical filter with automatic choice of foot-steps [29]. This will be done after implementing another stabilizer on the robot.

The current stabilizer, included in the walking pattern generator provided by PAL-Robotics, is considering the effects of all the structural compliances by estimating the trunk orientation with respect to the gravity field. Pyrene has structural compliances at the level of the hip, which are higher than the ones on HRP-2. However, compared to the HRP-2 compliance located at the ankles, the effect of this structural compliance on the CoP position is weaker. The disadvantage of not having a mechanical compliance to absorb impacts is the need to control accurately the robot dynamics. Our experience in tackling this issue is to have a walking pattern generator handling the robot dynamics. The strategy is to use it together with torque control to improve the walking performance.

B. Simulation: climbing stairs

In a previous work [15] the Gepetto Team has proposed an algorithm to plan the centroidal dynamics for a given set of contact points in the stairs. In a second phase an Operational Space Inverse Dynamics is used to compute the joint trajectory producing a dynamically consistent trajectory.

This algorithm has been successfully applied to HRP-2. We used the same algorithm on the URDF model of Pyrene . The results in simulation are depicted in Fig. 10.

V. CONCLUSION

In this paper we have presented a new humanoid robot with an actuation technology using electric motors. This humanoid tries to take the best in the field in terms of communication buses, motor size, reduction, kinematics and highly redundant sensing of the actuators for tackling industrial applications.

APPENDIX

The participation of the authors to the work described in this paper is the following: O. Stasse (Gepetto TEAM - Coordinator) , T. Flayols (Gepetto TEAM - Electrotechnics specialist) , R. Budhiraja (Gepetto TEAM - Multi-contact and tests on Pyrene) , K. Giraud-Esclasse (Gepetto TEAM - Mechanical specialist and tests on Pyrene) , J. Carpentier (Gepetto TEAM - Multi-contact on Pyrene) , A. Del Prete (Gepetto TEAM - Torque control on Pyrene) , P. Souères (Gepetto TEAM - Team leader) , N. Mansard (Gepetto TEAM - Motion control) , F. Lamiroux (Gepetto TEAM - Planning) , J.-P. Laumond (Gepetto TEAM - Project Actantrophe leader) , L. Marchionni (PAL Robotics - Mechatronics specialist) , H. Tome (PAL Robotics - Software and Motion Control) , F. Ferro (PAL Robotics - CEO)

ACKNOWLEDGMENT

This work was partially supported by the ERC-ADG 340050 Actantrophe and the CNRS Institute INSII.

REFERENCES

- [1] S. Lohmeier, T. Buschmann, and H. Ulbrich, "Humanoid robot lola," in *IEEE/RAS Int. Conf. on Robotics and Automation (ICRA)*, 2009.
- [2] F. Negrello, M. Garabini, M. G. Catalano, P. Kryczka, W. Choi, D. G. Caldwell, A. Bicchi, and N. G. Tsagarakis, "Walk-man humanoid lower body design optimization for enhanced physical performance," in *IEEE/RAS Int. Conf. on Robotics and Automation (ICRA)*, 2016, pp. 1817–1824.
- [3] K. Kojima, T. Karasawa, T. Kozuki, E. Kuroiwa, S. Yukizaki, S. Iwashita, T. Ishikawa, R. Koyama, S. Noda, F. Sugai, S. Nozawa, Y. Kakiuchi, K. Okada, and M. Inaba, "Development of life-sized high-power humanoid robot JAXON for real-world use," in *IEEE/RAS Int. Conf. on Humanoid Robotics (ICHR)*, 2015.

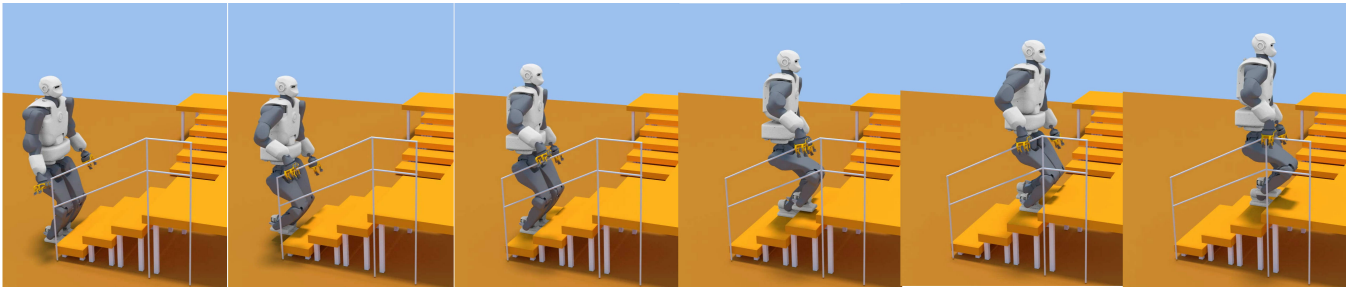


Fig. 10. Dynamical simulation of Pyrène climbing up stairs

- [4] S. R. Institute, "Proxi: Redefining humanoid efficiency," 2016. [Online]. Available: <https://www.sri.com/sites/default/files/brochures/proxi-humanoid-robot.pdf>
- [5] A. Hereid, E. A. Cousineau, C. M. Hubicki, and A. D. Ames, "3d dynamic walking with underactuated humanoid robots: A direct collocation framework for optimizing hybrid zero dynamics," in *IEEE/RAS Int. Conf. on Robotics and Automation (ICRA)*, 2016.
- [6] K. Kaneko, M. Morisawa, S. Kajita, S. Nakaoka, T. Sakaguchi, R. Cisneros, and F. Kanehiro, "Humanoid robot hrp-2 kai - improvement of hrp-2 towards disaster response tasks," in *IEEE/RAS Int. Conf. on Humanoid Robotics (ICHR)*, 2015, pp. 132–139.
- [7] Rainbow, "<http://www.rainbow-robotics.com/>," January 2017.
- [8] J. Engelsberger, A. Werner, C. Ott, B. Henze, M. A. Roa, G. Garofalo, R. Burger, A. Beyer, O. Eiberger, K. Schmid, and A. Albu-Schffer, in *IEEE/RAS Int. Conf. on Humanoid Robotics (ICHR)*, 2014.
- [9] J. Urata, Y. Nakanishi, and K. O. et M. Inaba, "Design of high torque and high speed leg module for high power humanoid," in *IEEE/RSJ Int. Conf. on Intelligent Robots and Systems (IROS)*, 2010.
- [10] N. A. Radford, P. Strawser, K. Hambuchen, J. S. Mehling, W. K. Verdeyen, A. S. Donnan, and al., "Valkyrie: Nasa's first bipedal humanoid robot," *Journal of Field Robotics*, vol. 32, no. 3, pp. 397–419, 2015.
- [11] N. Paine, J. S. Mehling, J. Holley, N. A. Radford, G. Johnson, C.-L. Fok, and L. Sentis, "Actuator control for the nasa-jsc valkyrie humanoid robot: A decoupled dynamics approach for torque control of series elastic robots," *Journal of Field Robotics*, vol. 32, no. 3, pp. 378–396, 2015.
- [12] S. Feng, X. Xinjilefu, C. G. Atkeson, and J. Kim, "Robust dynamic walking using online foot step optimization," in *IEEE/RSJ Int. Conf. on Intelligent Robots and Systems (IROS)*, 2016.
- [13] A. Sherikov, D. Dimitrov, and P.-B. Wieber, "Whole body motion controller with long-term balance constraints," in *IEEE/RAS Int. Conf. on Humanoid Robotics (ICHR)*, 2016.
- [14] S. Kuindersma, R. Deits, M. Fallon, A. Valenzuela, H. Dai, F. Permenter, T. Koolen, P. Marion, and R. Tedrake, "Optimization-based locomotion planning estimation and control design for the atlas humanoid robot," *Autonomous Robots*, vol. 40, pp. 429–455, 2015.
- [15] J. Carpentier, S. Tonneau, M. Naveau, O. Stasse, and N. Mansard, "A versatile and efficient pattern generator for generalized legged locomotion," in *IEEE/RAS Int. Conf. on Robotics and Automation (ICRA)*, 2016.
- [16] K. Kaneko, K. Harada, F. Kanehiro, G. Miyamori, and K. Akachi, "Humanoid robot hrp-3," in *IEEE/RSJ Int. Conf. on Intelligent Robots and Systems (IROS)*, 2008, pp. 2471–2478.
- [17] K. Kaneko, F. Kanehiro, M. Morisawa, K. Akachi, G. Miyamori, A. Hayashi, and N. Kanehira, "Humanoid robot hrp-4 - humanoid robotics platform with lightweight and slim body," in *IEEE/RSJ Int. Conf. on Intelligent Robots and Systems (IROS)*, 2011, pp. 4400–4407.
- [18] R. Tellez, F. Ferro, S. Garcia, E. Gomez, E. Jorge, D. Mora, D. Pinyol, J. Oliver, O. Torres, J. Velazquez, and D. Faconti, "Reem-b: An autonomous lightweight human-size humanoid robot," in *IEEE/RAS Int. Conf. on Humanoid Robotics (ICHR)*, 2008, pp. 462–468.
- [19] K. Mombaur, "Koroibot project fp 7 grant 611909," 2013. [Online]. Available: <http://orb.iwr.uni-heidelberg.de/koroibot/about-the-project/>
- [20] J. Mirabel, S. Tonneau, P. Fernbach, A.-K. Seppälä, M. Campana, N. Mansard, and F. Lamiroux, "Hpp: a new software for constrained motion planning," in *IEEE/RSJ Int. Conf. on Intelligent Robots and Systems (IROS)*, 2016.
- [21] M. Morisawa, K. Harada, S. Kajita, S. Nakaoka, K. Fujiwara, F. Kanehiro, K. Kaneko, and H. Hirukawa, "Experimentation of humanoid walking allowing immediate modification of foot place based on analytical solution," in *IEEE/RAS Int. Conf. on Robotics and Automation (ICRA)*, 2007, pp. 3989–3994.
- [22] K. Kaneko, F. Kanehiro, S. Kajita, H. Hirukawa, T. Kawasaki, M. Hirata, K. Akachi, and T. Isozumi, "Humanoid robot HRP-2," in *IEEE/RAS Int. Conf. on Robotics and Automation (ICRA)*, 2004, pp. 1083–1090.
- [23] M. Focchi, G. Medrano-Cerda, T. Boaventura, M. Frigerio, C. Semini, J. Buchli, and D. G. Caldwell, "Robot impedance control and passivity analysis with inner torque and velocity feedback loops," *Control Theory and Technology*, vol. 14, no. 2, pp. 97–112, 2016.
- [24] F. Negrello, M. Garabini, M. Catalano, J. Malzahn, D. Caldwell, A. Bicchi, and N. Tsagarakis, "A modular compliant actuator for emerging high performance and fall-resilient humanoids," in *IEEE/RAS Int. Conf. on Humanoid Robotics (ICHR)*, 2015.
- [25] J. Urata, J. Urata, T. Hirose, Y. Namiki, Y. Nakanishi, I. Mizuuchi, and M. Inaba, "Thermal control of electrical motors for high-power humanoid robots," in *IEEE/RSJ Int. Conf. on Intelligent Robots and Systems (IROS)*, 2008.
- [26] M. F. Fallon, P. Marion, R. Deits, T. Whelan, M. Antone, J. McDonald, and R. Tedrake, "Continuous humanoid locomotion over uneven terrain using stereo fusion," in *IEEE/RAS Int. Conf. on Humanoid Robotics (ICHR)*, 2015.
- [27] N. Mansard, O. Stasse, P. Evrard, and A. Kheddar, "A versatile generalized inverted kinematics implementation for collaborative working humanoid robots: The stack of tasks," in *International Conference on Advanced Robotics (ICAR)*, June 2009, p. 119.
- [28] N. Ando, T. Suehiro, K. Kitagaki, T. Kotoku, and W.-K. Yoon, "Rt-middleware: distributed component middleware for rt (robot technology)," in *IEEE/RSJ Int. Conf. on Intelligent Robots and Systems (IROS)*, 2005.
- [29] M. Naveau, M. Kudruss, and O. Stasse, "A reactive walking pattern generator based on nonlinear model predictive control," *IEEE/RAS Robotics and Automation Letters*, 2016.